Contents lists available at ScienceDirect

Comparative Biochemistry and Physiology, Part A

CO$_2$ induced seawater acidification impacts sea urchin larval development I: Elevated metabolic rates decrease scope for growth and induce developmental delay

M. Stumpp [a], J. Wren [b], F. Melzner [a], M.C. Thorndyke [c], S.T. Dupont [b,*]

[a] Biological Oceanography, Leibniz Institute of Marine Sciences (IFM-GEOMAR), 24105 Kiel, Germany
[b] Department of Marine Ecology, Sven Lovén Centre for Marine Sciences, Kristineberg, University of Gothenburg, Sweden
[c] The Royal Swedish Academy of Sciences, Sven Lovén Centre for Marine Sciences, Kristineberg, University of Gothenburg, Sweden

ARTICLE INFO

ABSTRACT

Anthropogenic CO$_2$ emissions are acidifying the world's oceans. A growing body of evidence is showing that ocean acidification impacts growth and developmental rates of marine invertebrates. Here we test the impact of elevated seawater pCO$_2$ (129 Pa, 1271 µatm) on early development, larval metabolic and feeding rates in a marine model organism, the sea urchin *Strongylocentrotus purpuratus*. Growth and development was assessed by measuring total body length, body rod length, postoral rod length and posterolateral rod length. Comparing these parameters between treatments suggests that larvae suffer from a developmental delay (by ca. 8%) rather than from the previously postulated reductions in size at comparable developmental stages. Further, we found maximum increases in respiration rates of + 100% under elevated pCO$_2$, while body length corrected feeding rates did not differ between larvae from both treatments. Calculating scope for growth illustrates that larvae raised under high pCO$_2$ spent an average of 39 to 45% of the available energy for somatic growth, while control larvae could allocate between 78 and 80% of the available energy into growth processes. Our results highlight the importance of defining a standard frame of reference when comparing a given parameter between treatments, as observed differences can be easily due to comparison of different larval ages with their specific set of biological characters.

© 2011 Elsevier Inc. All rights reserved.

1. Introduction

Anthropogenic release of atmospheric CO$_2$ leads to ocean warming and acidification. This has been proposed as a major threat for marine organisms, in particular calcifying organisms (Orr et al., 2006; Doney et al., 2009). However, ocean acidification research is a new field and relatively little experimental evidence is available on the potential impacts on marine biota (Kroeker et al., 2010).

Sea urchins have been used widely as model organisms in developmental biology, cell and evolutionary biology and toxicology for decades. Among the studied species, the purple sea urchin, *Strongylocentrotus purpuratus*, with a sequenced genome (The Sea Urchin Genome Sequencing Consortium, 2006), is the most widely used. Owing to the extensive knowledge accumulated on the timing of embryonic and larval development (Smith et al., 2008), as well as the underlying gene regulatory networks (Ben-Tabou de-Leon and Davidson, 2007), this species is an excellent candidate to study the effects of abiotic stressors such as elevated seawater pCO$_2$ on the normal progression of larval development.

S. purpuratus is a long lived species (up to 50 years, Ebert, 1967) and an abundant and key component of the intertidal and sub-tidal zone of the Eastern Pacific coast, with a distribution range from Mexico to Alaska (Biermann et al., 2003) and an important fishery resource. It is an important grazer of macroalgae, particularly kelp, and it competes with other grazers (abalone, *Haliotis* spp., red sea urchin *Strongylocentrotus franciscanus*) and is a food source for many predators including sea otters (Steneck et al., 2002). Sea urchins are a central element in the structure of the marine benthic community. For example, a delicate balance between sea urchin grazing pressure and kelp forest productivity leads to stable states that alternate between kelp forest and sea urchin "barrens" (Pearse, 2006). In addition to competition, predation and food limitation, sea urchin abundance is heavily influenced by recruitment intensity. It is thus of primary importance to understand how climate change might impact larval recruitment in important keystone species such as *S. purpuratus* (Dupont et al., 2010c).

A growing body of evidence indicates that ocean acidification might impact growth, calcification and developmental rates in echinoderm species (Dupont et al., 2010c). While the lecitotroph echinoderm larvae *Crossaster papposus* showed elevated growth rates (Dupont et al., 2010b) when raised under elevated pCO$_2$ (ca. 120 Pa, 1184 µatm, pH 7.7), sea urchin planktotrophic larval stages from

* Corresponding author at: Department of Marine Ecology, Sven Lovén Centre for Marine Sciences, Kristineberg 566, 45034 Fiskebäckskil, Sweden.
E-mail address: sam.dupont@marecol.gu.se (S.T. Dupont).

several species appears to be smaller at a given time post-fertilization and/or grow more slowly (see Dupont et al., 2010c for review). However, it is unclear, whether observed growth reductions are due to a reduction in the ability to calcify at high rates or to other factors such as limitations in feeding ability. Although Martin et al. (2011) found that *Paracentrotus lividus* larvae are characterized by a fully developed skeleton when normalized to body length, calcification of the larval skeleton, which comprises a framework of spicules made of $CaCO_3$ (highly soluble Mg Calcite form, Okazaki and Inoué, 1976), might be more costly due to low extracellular matrix pH and high extracellular matrix pCO_2. In addition, maintenance of intracellular pH and general cellular homeostasis might require additional energy (Deigweiher et al., 2010). Thus, growth reductions in larval echinoderm species might be indirect effects of an altered partitioning of the energy budget. Similar conclusions have been reached by Thomsen and Melzner (2010) where increased metabolic rates in high pCO_2 acclimated bivalves (blue mussel *Mytilus edulis*) were accompanied by reduced rates of calcification and growth.

Under the hypothesis that the main CO_2 effect visible on the larval organism level would be reduced speed of development, ultimately caused by energy budget constraints, investigating the impact of elevated pCO_2 on larval development would create a classic experimental design problem that has been poorly addressed by ocean acidification experiments on echinoderm larval stages so far: any biological parameter of interest, at a given time point in an experiment might be severely confounded by differences in development between treatment groups. For example, it is known from the extensive study of echinoderm developmental gene regulatory networks that expression patterns of genes and associated physiological function are highly variable yet precisely structured chronologically (Ben-Tabou de-Leon and Davidson, 2007). As a consequence, age or time post-fertilization would then not be the right reference scale to discuss effects of elevated seawater pCO_2 on biological processes of interest. Any observed effect at a given time may just be a consequence of a delay in development (Pörtner et al., 2010).

We hypothesize that elevated seawater pCO_2 primarily impacts the energy budget, which then leads to reduced rates of development. The aim of this paper is to test this hypothesis and investigate the impact of elevated seawater pCO_2 on *S. purpuratus* larval survival, development, growth, aerobic metabolic rate and feeding rate. The data will be used to combine respiration and feeding data to calculate scope for growth (SfG), a measure of energy balance, and will be correlated and compared to the observed growth rates. In a companion paper (Stumpp et al., 2011), we use an explorative gene expression approach to analyze key physiological processes that might impact the larval energy budget.

2. Material and methods

2.1. Animal collection

Adult *Strongylocentrotus purpuratus* were collected on the Californian coast (Kerckoff Marine Laboratory, California Institute of Technology, USA) and transferred to the Sven Lovén Centre for Marine Science (Kristineberg, Sweden). They were maintained in natural flowing seawater at 14 °C and pH 8.1 on a diet of *Ulva lactuca*.

2.2. Larval culture and experimental conditions

Spawning was induced in June–July 2008 and 2009 by intracoelomic injection of 0.5 M KCl in filtered seawater (FSW). In each experiment, gametes from three males and three females were used. After fertilization, cleaving embryos (two cells stage) were placed in 5 L (survival, growth and feeding) or 50 L (respiration) aquaria filled with FSW at a density of 5 to 10 embryos per mL at a temperature of 14 °C. Larger culture vessels for metabolic rate experiments were needed due to the high amount of larvae required for respiration trials (>2000 larvae per time point). The FSW was continuously aerated to maintain oxygen concentrations close to air saturation and mixed by the slow convective current of a stream of single bubbles (approx. 100 bubbles per min). After 5 days, larvae were fed daily with the cryptophyte algae *Rhodomonas* sp. which were raised in B1 medium (Guillard and Ryther, 1962) at 20 °C under a 12:12 h light:dark cycle. Algal strains were provided by the Marine Algal Culture Centre at Gothenburg University (GUMACC). Larvae were fed at a constant concentration of 150 µg C L^{-1}. The carbon content of the algae was estimated based on biovolume measurements as equivalent spherical diameter (ESD) with an electronic particle analyzer (Elzone 5380, Micrometrics, Aachen, Germany) and equations provided by Mullin et al. (1966). To prevent changes in food concentration, algae concentration and size were checked daily using a coulter counter (Elzone 5380, Micrometrics, Aachen, Germany) and then adjusted in the experimental bottles to the maximum concentration of 150 µg carbon L^{-1} (~3000 to 6000 cells mL^{-1} for diameters ranging between 6 and 8 µm). At the chosen algae concentration, seawater pCO_2 treatment levels and temperatures had no impact on algal growth and survival (result not shown).

Cultures were maintained at a salinity of 32‰ and a total alkalinity of 2200 ± 30 µmol kg^{-1} as measured following Sarazin et al. (1999). The carbonate system speciation (pCO_2, Ω_{Ca} and Ω_{Ar}) was calculated from pH and alkalinity using CO2SYS (Lewis and Wallace, 1998, Table 1) with dissociation constants from Mehrbach et al. (1973) refitted by Dickson and Millero (1987). Our treatments were control/natural seawater (pH = 8.1, pCO_2 38 Pa, 375 µatm, T = 14 °C) and high seawater pCO_2 (pH = 7.7, pCO_2 128 Pa, 1264 µatm, T = 14 °C). pH was maintained in each aquarium using a computerized feedback system (AquaMedic) that regulates pH (NBS scale) by addition of pure gaseous CO_2 directly into the seawater (+/−0.02 pH units). Three replicates (n = 3) were used for 5 L cultures (morphology) and two replicates (n = 2) for the 50 L cultures (respiration).

2.3. Mortality and growth

Larval cultures were monitored daily for 21 days. Each day, 3 subsamples of more than 50 larvae was removed from each culture and fixed in buffered 4% paraformaldehyde (PFA) in FSW for later analysis. Density at time t (Nt in larvae L^{-1}) was estimated by dividing the number of larvae by the corresponding volume collected. For each replicate, 10 fixed larvae were photographed every (1 to 7 days post-fertilization) or every other day (after 7 days post-fertilization) with a digital camera mounted on a dissecting microscope using polarized light to visualize the skeleton. Five morphometric parameters (body length, body rod lengths (right and left), postoral rod lengths and posterolateral rod length, Fig. 1)

Table 1
Carbonate system speciation in the experimental treatments. Total dissolved inorganic carbon (C_T), pCO_2 and calcium carbonate saturation state for aragonite and calcite (ΩCa, ΩAr) were calculated from pH_{NBS} and A_T.

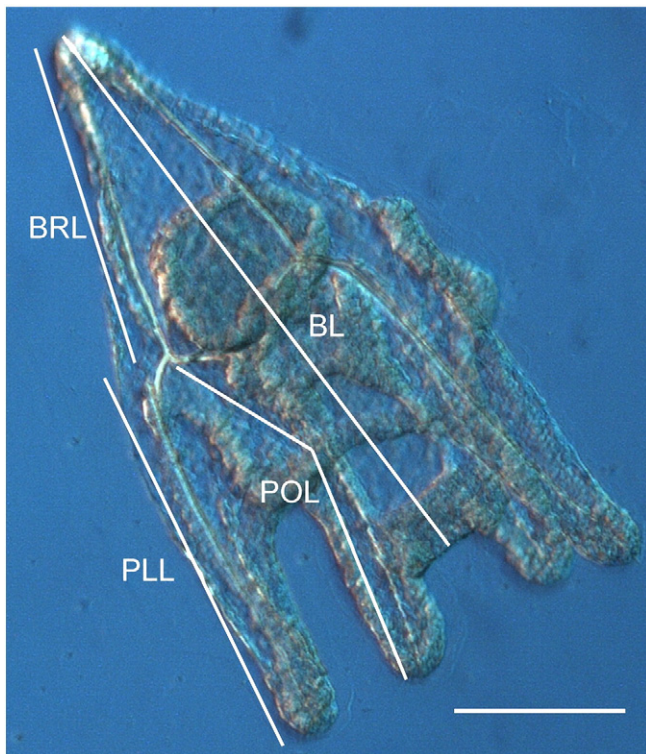| pH_{NBS}	A_T (µmol/kg SW)	S	T (°C)	pCO_2 (Pa)	C_T (µmol/kg SW)	ΩCa	ΩAr
8.18 ± 0.02	2200 ± 30	32	14	38 ± 3	2002 ± 37	3.42 ± 0.08	2.18 ± 0.05
7.70 ± 0.02	2200 ± 30	32	14	128 ± 8	2170 ± 36	1.27 ± 0.04	0.81 ± 0.02

Fig. 1. Morphometric coordinates and morphology of a *Strongylocentrotus purpuratus* 4-arm pluteus larva. BL, body length; BRL, body rod length; PLL, posterolateral arm length; POL, post-oral rod length. Scale bar 50 μm.

were measured for each larva using LAS software (Leica). A symmetry index was calculated as the ratio of left to right overall length.

2.4. Antibody labeling

Antibody labeling was used to visualize the larval endoskeleton (Primary mesenchyme cells, PMC, revealed by a PMC-specific cell surface marker, Anstrom et al., 1987) and the nervous system (serotonin). At 3 days post-fertilization, larvae were fixed in 4% PFA in FSW for 15 min, then post-fixed with ice-cold methanol for 1 min at room temperature (RT). Fixed specimen were rinsed 3 times in phosphate-buffered saline (PBS) pH 7.4 and then blocked for 2 h in 4% bovine albumin serum containing 0.1% tween-20 at RT. Anti-serotonin (Sigma) and anti-MSP130 (a gift from Dave McClay, Duke University, USA) were diluted 1:500 in PBS. After overnight incubation (RT), embryos and larvae were rinsed at least 4 times in PBS then incubated in a 1:1000 dilution of Alexa488 conjugated anti-rabbit IgG and Alexa568 conjugated anti-mouse IgG (Molecular Probes). After incubation (2 h, RT), embryos and larvae were rinsed 4 times in PBS. Specimens were mounted in PBS, examined using a Leica confocal microscope (SP5) and analyzed by collecting stacks of images and projecting them in the Y-axis.

2.5. Feeding

To assess the impact of elevated seawater pCO_2 on feeding performance, feeding rate was estimated every other day beginning at day 6 (commencement of feeding). 15 larvae each were transferred to 100 mL glass bottles (7 replicates) with food suspension (*Rhodomonas* sp. at 150 μg C L^{-1}) in FSW equilibrated with the same pCO_2 the respective experimental animals originated from (pH 8.1 or pH 7.7). Two sets of control bottles (3 replicates for each treatment) without larvae containing the same food suspension were also prepared. The bottles were incubated on a rotating plankton wheel

(0.2 rpm) at 14 °C. Feeding rate was estimated as clearance rate by measuring the algal concentration (delta cells L^{-1}) at the end of the incubation (24 h) in control and experimental bottles after collection of the larvae on a 50 μm sieve. As nutritional values of algae differ with size, algae cell size was simultaneously measured and feeding rate was expressed in changes in ng C L^{-1}. Feeding rate (F, mL ind^{-1} d^{-1}) was calculated following Frost (1972), and ingestion (I, cell volume ind^{-1} d^{-1}) was calculated as I = F × C, where C is the average algal concentration per bottle. Rates were corrected for mortality and are given as rates per surviving animal in ng C ind^{-1} h^{-1}.

2.6. Aerobic metabolic rate determinations

Respiration experiments were conducted every other day beginning at day 3 according to Marsh and Manahan (1999) with modifications. Briefly, respiration vials with volumes between 1624 and 1641 μl were placed in a water bath at 14 °C and filled with sterile filtered seawater (0.2 μm FSW, 14 °C) adjusted to control pH (pH 8.1) and low pH (pH 7.7). Larvae were washed three times with FSW of the appropriate pH of their rearing conditions to remove as much culture water as possible and were then transferred in a known volume of "transfer water" into the vials with their culture pH. Depending on stage, 48 to 724 larvae were placed into one vial. For replication, 10 vials were used for larvae of the same culture (two cultures per treatment, four cultures in total, forty vials with larvae in total per time point). Different numbers of larvae were placed into the vials for density controls as suggested by Marsh and Manahan (1999). Aerobic respiration rate increased linearly with increasing amounts of larvae in the vials. As no density effect was detected and in order to show the variability within larval cultures, we regarded each vial as a sub-replicate of each culture (true replicate) and used replicate cultures as co-variable in the statistical procedure. Several vials (n = 4 to 8 per measurement point) without larvae were prepared for bacterial controls. Bacterial controls were conducted according to Marsh and Manahan (1999). After addition of larvae or larval-free "transfer seawater" (bacterial control) to the vials, pO_2 was measured in all vials before closure with micro-optodes calibrated as suggested in the manufacturers manual (PreSens, 4-OXY Micro, Germany). Closed vials were then incubated horizontally submerged in the waterbath for 7 to 10 h in the dark. Continuous pO_2 measurements (n = 2 to 4) were conducted additionally in order to demonstrate a linearity of pO_2 decline in the respiration vials during the incubation time (data not shown). No changes in oxygen consumption rates during incubations were detected. After incubation, pO_2 was measured again and corrected for bacterial respiration. Following pO_2 measurement in the vials, larvae were pelleted by hand centrifugation, removed from the bottom of the vials and fixed in 4% PFA in seawater for enumeration. Respiration in bacterial controls did not exceed 15% of larval respiration and pO_2 in the vials did not drop below 80% air saturation. Larvae were counted subsequently to oxygen consumption measurements. Prior to fixation for counting, larvae were checked for viability.

To control the effect of pCO_2 in respiration experiments, the pH drop due to respiratory CO_2 excretion of the larvae was measured directly in the vials before and after incubation with a pH meter (WTW 340i pH meter and Sentix 80 electrode calibrated with Radiometer NIST precision buffers) in preliminary experiments. A mean pH drop of 0.1 units (standard deviation of 0.04 units) occurred during incubation, but there was no difference between pH decreases of the two pH treatments.

2.7. Scope for growth calculations

For calculation of scope for growth (SfG), metabolic and feeding rates (regressions vs. time post-fertilization, TPF) were used to estimate daily energy input and respiratory energy loss starting at

6 days TPF by conversion of metabolic and feeding rates to energy equivalents. Metabolic rates were converted to energy equivalents (484 µJ nmol^{-1} O$_2$, Gnaiger, 1983) based on oxyenthalpic values of lipid and protein as major constituents of echinoderm larvae (Shilling and Manahan, 1994). Larval clearance rate was converted to energy equivalents (1.34 10^5 µJ µg C^{-1}) using 19 µJ ng^{-1} *Rhodomonas* and a cell mass of 0.15 ng cell^{-1} as an estimate for our strain of *Rhodomonas* sp. (Renaud et al., 2002). Our *Rhodomonas* sp. population is characterized by an average diameter of 6.38 µm and a carbon content of 0.021 ng C cell^{-1}. SfG was then calculated from energy intake (I) and respiratory energy loss (R) as SfG = I − R.

SfG is displayed as energy available for development and is thus plotted against body length as standardization for larval morphometrics. For the calculation of the energy budget model, we assumed that larvae are 8.0% smaller under elevated pCO_2 conditions than under control conditions, demonstrated by the morphometric measurements in this study.

As excretion rates are difficult to determine in sea urchin larval stages, energy loss due to excretion was omitted from the analyses. One should bear in mind that this may possibly lead to an overestimation of SfG.

2.8. Statistical analysis

Simple linear and exponential regression models were used to test the relationship type between the variables. Analysis of co-variance (ANCOVA) was used to test for pCO_2 effects on the tested variable using TPF or body length (BL) as co-variable. When exponential relationships were calculated, TPF and BL were logarithm transformed. For testing for different routine metabolic rates in embryonic stages (day 3 to 5 PF), a Two-way ANOVA was performed with time and pH as variables. The Shapiro–Wilk test (Shapiro and Wilk, 1965) was used to check that the data were normally distributed and the Levene test was used to check that variances were homogenous. All statistical analyses were performed using SAS/STAT® software (SAS Institute, 1990). For clarity, regression equations, coefficients and statistics are listed in Table 2. ANCOVA results are listed in Table 3.

3. Results

3.1. Impact of seawater pCO_2 on larval survival

Normalized larval density in experimental cultures decreased with TPF following significant linear relationships (Fig. 2A) and relative densities (RD) were estimated from the slope of the regression. Daily mortality rate (DMR) was significantly (Table 3) higher under control conditions (DMR = 2.7 ± 0.2% d^{-1}) in comparison to that under high seawater pCO_2 (DMR = 2.2 ± 0.3% d^{-1}). When normalized against body length (BL; Fig. 2B), survival was still significantly higher in the high pCO_2 treatment than that in the control treatment (Table 3).

3.2. Impact of seawater pCO_2 on larval growth

Elevated seawater pCO_2 had an impact on the chronology of development. The 4-arm pluteus stage was reached (100% of the larvae) after 2 days under control conditions and after 3 days in the high pCO_2 treatment. A similar trend was observed in larval growth (BL, Fig. 3A). Within the time frame of the experiment, BL growth followed a logarithmic relationship (Table 2). In comparison to the control condition, increasing seawater pCO_2 had a significant negative impact on growth with no significant effects between replicates (Table 3). As a consequence, at a given time, larvae were significantly different in size and larvae reached the same size at different times (Fig. 3).

Table 2

Results of the regression analysis of measured parameters in *S. purpuratus* larvae raised under control (pH 8.1) and elevated pCO_2 conditions (pH 7.7): relative density (RD), larval body morphometrics (BL body length, BRL body rod length, PLL posterolateral rod length, POL postoral rod length), routine metabolic rates (RMR) and feeding rates (FR) relative to time post-fertilization (TPF) and body length (BL).

Parameter	Regression	R^2	df	F	p
RD vs TPF					
pH 8.1	RD = − 2.7 TPF + 97.2	0.58	1, 61	82.7	<0.001
pH 7.7	RD = − 2.2 TPF + 101.7	0.75	1, 61	179.2	<0.001
RD vs BL					
pH 8.1	RD = − 0.17 BL + 1.28	0.51	1, 61	63.4	<0.001
pH 7.7	RD = − 0.15 BL + 1.25	0.61	1, 61	94.7	<0.001
BL vs TPF					
pH 8.1	BL = 111.05 ln(TPF) + 111.71	0.96	1, 388	905.2	<0.001
pH 7.7	BL = 103.78 ln(TPF) + 105.05	0.96	1, 388	828.6	<0.001
BRL vs TPF					
pH 8.1	BRL = 81.96 ln(TPF) + 52.22	0.92	1, 358	1411.8	<0.001
pH 7.7	BRL = 76.92 ln(TPF) + 49.28	0.90	1, 358	1353.9	<0.001
BRL vs BL					
pH 8.1	BRL = 0.58 BL + 29.15	0.96	1, 358	6649.5	<0.001
pH 7.7	BRL = 0.58 BL + 26.28	0.96	1, 358	10949.0	<0.001
PLL vs TPF					
pH 8.1	PLL = 98.88 ln(TPF) + 8.46	0.96	1, 358	954.0	<0.001
pH 7.7	PLL = 91.87 ln(TPF) + 7.16	0.96	1, 358	624.4	<0.001
PLL vs BL					
pH 8.1	PLL = 0.81 BL − 68.74	0.96	1, 358	6333.9	<0.001
pH 7.7	PLL = 0.83 BL − 70.52	0.95	1, 358	7476.7	<0.001
POL vs TPF					
pH 8.1	POL = 74.68 ln(TPF) − 0.82	0.92	1, 358	616.6	<0.001
pH 7.7	POL = 71.55 ln(TPF) − 6.54	0.93	1, 356	575.1	<0.001
POL vs BL					
pH 8.1	POL = 0.62 BL − 62.55	0.88	1, 358	3829.5	<0.001
pH 7.7	POL = 0.68 BL − 80.66	0.96	1, 356	6175.0	<0.001
FR vs TPF					
pH 8.1	FR = 0.52 TPF − 1.38	0.50	1, 45	45.5	<0.001
pH 7.7	FR = 0.27 TPF − 0.46	0.42	1, 61	44.7	<0.001
FR vs BL					
pH 8.1	FR = 0.05 BL − 13.05	0.48	1, 45	42.1	<0.001
pH 7.7	FR = 0.03 BL − 8.12	0.43	1, 61	46.2	<0.001
RMR vs TPF					
pH 8.1	RMR = 1.09 TPF + 4.76	0.80	1, 156	639.7	<0.001
pH 7.7	RMR = 2.18 TPF − 4.98	0.87	1, 154	1074.9	<0.001
RMR vs TPF					
pH 8.1	RMR = 0.13 BL − 30.38	0.80	1, 156	637.5	<0.001
pH 7.7	RMR = 0.27 BL − 73.42	0.85	1, 154	884.4	<0.001

Similar significant relationships were also observed for other morphometric parameters (body (BRL), post-oral (POL) and posterolateral (PLL) rod lengths; Fig. 4, Table 2) with significant differences between pCO_2 treatments as revealed by analysis of covariance with no significant differences between replicate cultures (Table 3). Differences in morphology between the pCO_2 treatments vanished when plotted against BL rather than TPF (Table 3). This indicates that observed larval morphometric differences between treatments on given sampling days were a consequence of a delay in development.

Overall, the symmetry index was high (average SI = 0.97 ± 0.001, minimum = 0.90) and was not correlated to neither TPF nor BL. No difference was observed between pCO_2 treatments or replicates (Figure S1 supplementary material, TPF: F = 1.34, p<0.23; BL: F = 1.38, p<0.22).

3.3. Impact of seawater pCO_2 on larval morphology

The nervous system was labeled in 3 day old larvae using an anti-serotonin antibody (in red, Fig. 5). The nervous system was normally developed in all treatments with regard to development stage (Bisgrove and Burke, 1986). Anti-serotonin immunoreactivity occurs in cells organized in an apical ganglion at the apical plate. In both treatments nerve cells extend fine cellular processes. Skeletal morphology was revealed by the PMC-specific cell surface marker, MSP130 (in green, Fig. 5), in 3 day pluteus larvae. Skeletal rod

Table 3
Analysis of covariance (ANCOVA) results of measured parameters in *S. purpuratus* larvae raised under control (pH 8.1) and elevated pCO_2 conditions (pH 7.7): relative density (RD), larval body morphometrics (BL body length, BRL body rod length, PLL posterolateral rod length, POL postoral rod length), routine metabolic rates (RMR) and feeding rates (FR) relative to time post-fertilization (TPF) and body length (BL).

Parameter	Source	df	F	p
RD vs TPF	Model	1, 123	115.1	<0.001
	pH	1	20.7	<0.001
	Time	1	209.4	<0.001
RD vs BL	Model	1, 123	80.92	<0.001
	pH	1	4.3	<0.05
	Time	1	209.4	<0.001
BL vs TPF[a]	Model	5, 773	292.8	<0.001
	pH	1	28.6	<0.001
	Time	1	1727.0	<0.001
	Replicate	4	0.3	=0.87
BRL vs TPF[a]	Model	5, 713	479.7	<0.001
	pH	1	114.9	<0.001
	Time	1	2761.1	<0.001
	Replicate	4	0.6	=0.69
BRL vs BL	Model	5, 713	2903.6	<0.001
	pH	1	1.6	=0.12
	Time	1	16720.2	<0.001
	Replicate	4	1.0	=0.40
PLL vs TPF[a]	Model	5, 713	261.6	<0.001
	pH	1	40.8	<0.001
	Time	1	1524.1	<0.001
	Replicate	4	1.17	=0.32
PLL vs BL	Model	5, 713	2457.7	<0.001
	pH	1	0.96	=0.33
	Time	1	14282.7	<0.001
	Replicate	4	1.0	=0.41
POL vs TPF[a]	Model	5, 771	201.3	<0.001
	pH	1	39.5	<0.001
	Time	1	1166.3	<0.001
	Replicate	4	0.81	=0.52
POL vs BL	Model	5, 771	1619.6	<0.001
	pH	1	0.27	=0.60
	Time	1	9370.9	<0.001
	Replicate	4	2.8	=0.06
FR vs TPF	Model	1, 107	46.1	<0.001
	pH	1	33.0	<0.001
	Time	1	78.2	<0.001
FR vs BL	Model	1, 107	49.7	<0.001
	pH	1	4.62	=0.054
	Time	1	84.81	<0.001
RMR vs TPF	Model	3, 309	304.7	<0.001
	pH	1	142.4	<0.001
	Time	1	1073.4	<0.001
	Replicate	2	2.42	=0.09
RMR vs TPF	Model	3, 309	253.7	<0.001
	pH	1	470.8	<0.001
	Time	1	888.8	<0.001
	Replicate	2	2.0	=0.13

[a] On log transformed data.

development appeared normal in both pCO_2 treatments (Yajima and Kiyomoto, 2006).

3.4. Impact of pCO_2 on feeding

Feeding rate (FR) increased with TPF following significant linear relationships (Fig. 6A, Table 2). FR was significantly (Table 3) higher under control conditions when compared to high pCO_2 (Table 2). However, when plotted against BL (Fig. 6B), FR in the high pCO_2 did not significantly differ from the control (Table 3).

3.5. Impact of seawater pCO_2 on aerobic metabolic rates

Routine metabolic rates (RMR) were measured in larvae raised at pH 8.1 and 7.7. In embryonic stages (blastula, gastrula) and prism larval stages, RMR was constant, ranging from 6.9 to 10.4 pmol O_2 ind^{-1} h^{-1} (Fig. 7). There was no significant effect of seawater pCO_2
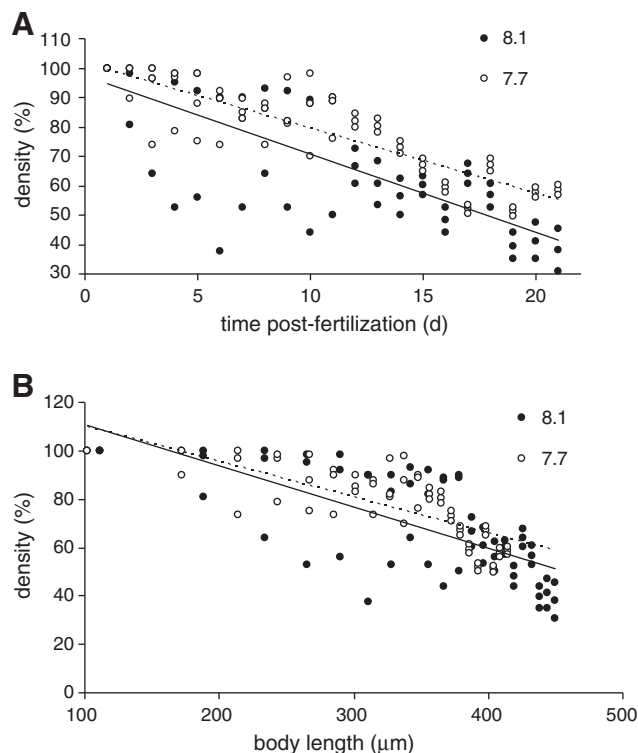

Fig. 2. Relative density of larvae in triplicate cultures under control (black symbols, solid regression, pH = 8.1, pCO_2 38 Pa) and elevated pCO_2 (open symbols, dashed regression, pH = 7.7, pCO_2 128 Pa) plotted against time post-fertilization (TPF, A) and body length (BL, B). If only two data points are visible, data points overlap. Mortality plotted against TPF and body length differs significantly between treatments (Table 3). Regression equations and coefficients are listed in Table 2.

on RMR during embryonic development. Upon feeding (>5 days TPF), RMR increased linearly from 11.2 and 10.4 (day 7) to 29.0 and 41.9 pmol O_2 ind^{-1} h^{-1} (day 21) under control conditions and elevated pCO_2 conditions, respectively (Fig. 7A, Table 2). No significant effect between replicate cultures was detected (Table 3). The ontogenetic rate of increase in RMR under elevated pCO_2 was significantly (2 times) greater than that under control conditions when TPF was considered (Table 3). When related to body length, RMR also increased linearly (Fig. 7B, Table 2) and the increase in
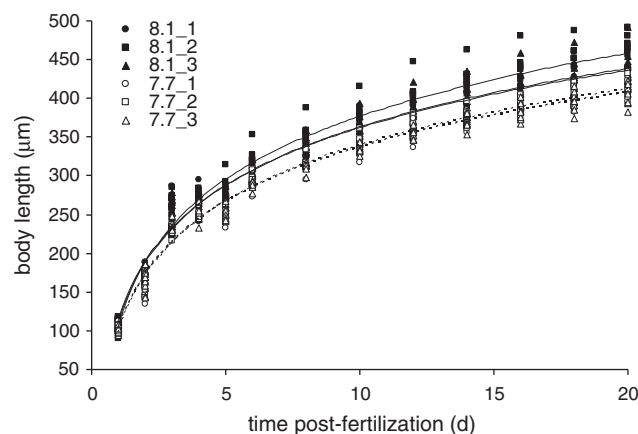

Fig. 3. Growth of body length (BL) of triplicate cultures (pH 8.1 black symbols and solid regression, pH 7.7 open symbols and dashed regression) plotted against time post-fertilization. Regressions differ significantly between treatments (Table 3). Regression equations and coefficients are listed in Table 2.
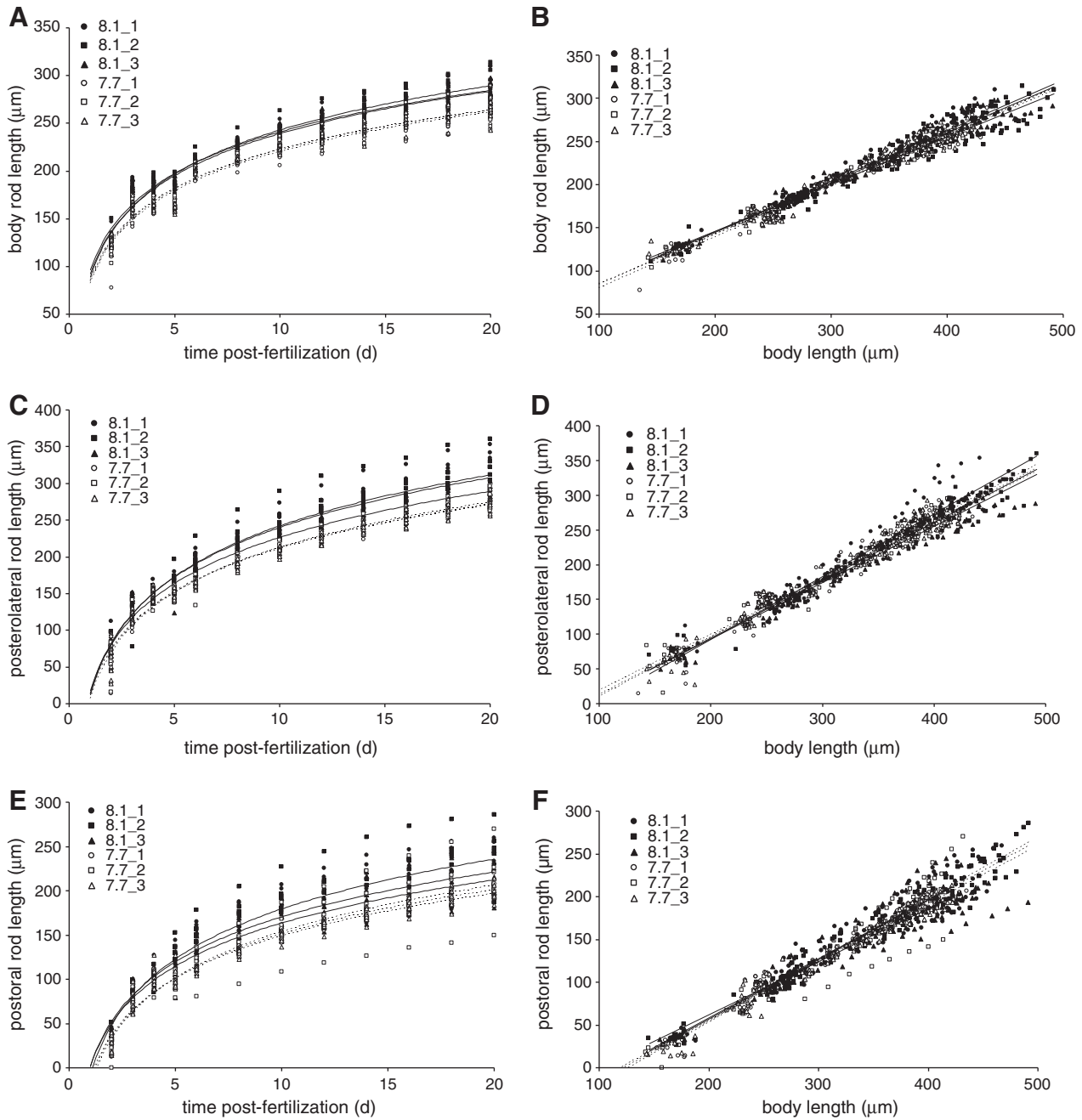
Fig. 4. Individual growth of 3 measured morphometric parameters in triplicate cultures (body rod length, BRL; posterolateral rod length, PLL and postoral rod length, POL, μm) plotted against time post-fertilization (A, C, E) and body length (B, D, F). See Fig. 1 for definition of the parameters. Significant differences between control (black symbols, solid regression) and elevated pCO$_2$ (open symbols, dashed regression) treatments were only observed, when morphometrics were plotted against time post-fertilization (Table 3). For clarity reasons, regression equations and coefficients are listed in Table 2.

respiration was significantly higher (2.1 times) under hypercapnic conditions (Table 3). The variability in RMR between low pH cultures was higher than in cultures maintained under control conditions.

3.6. Impact of seawater pCO$_2$ on scope for growth

For larval development of *S. purpuratus* under control and elevated pCO$_2$, scope for growth (SfG) was estimated using energy intake through feeding and respiratory energy loss versus larval size (body length). SfG of larvae raised under control conditions increased during larval growth from 19 μJ at a body length of 310 μm to 53 μJ at a body length of 449 μm (Fig. 8A). SfG of larvae raised at elevated pCO$_2$ was

reduced and showed a weaker increase during development, with values between 3 μJ at a body length of 287 μm and 13 μJ at a body length of 416 μm. SfG relative to energy input (SfG$_{\%I}$) increased slightly in control conditions from 78% to 80% over development. Under high pCO$_2$ conditions, SfG$_{\%I}$ was generally lower than under control conditions and decreased during development with values between 45% and 39% (Fig. 8B). By dividing SfG by the daily growth in body length (SfG$_{BL}$) at a given body length, we estimated the energy that is available in *S. purpuratus* larvae to grow a certain size increment (μm) during development. SfG$_{BL}$ increases exponentially in both treatments but steeper under control conditions: at 330 μm size larvae raised under control conditions have 30 μJ to grow another μm,
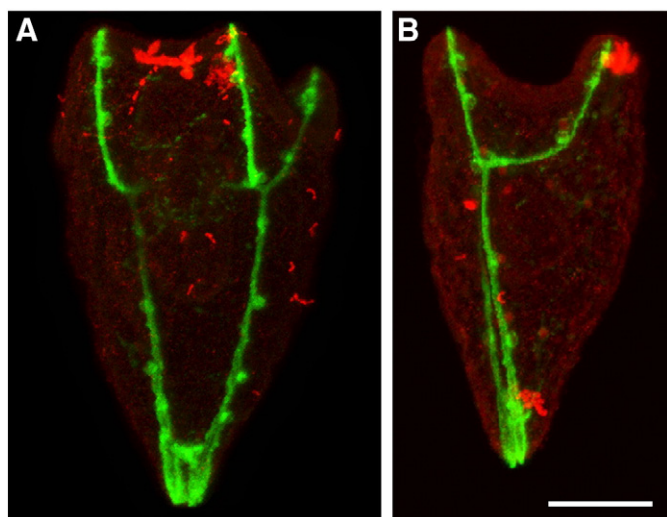
Fig. 5. Confocal laser scanning images of the larval endoskeleton (primary mesenchyme cells − PMC) and nervous system, using PMC-specific cell surface antibody, MSP130 (green), and anti-serotonin (red) antibodies, in 4-arm pluteus stage of *Strongylocentrotus purpuratus* larvae raised under control (A, dorsal view) and elevated pCO_2 conditions (B, left side). Scale bar for A and B with 50 μm.

while larvae under elevated pCO_2 only have 10 μJ. At a size of 415 μm the larvae are supplied with 110 and 50 μJ to grow 1 μm in length for control and elevated pCO_2, respectively (Fig. 8C).
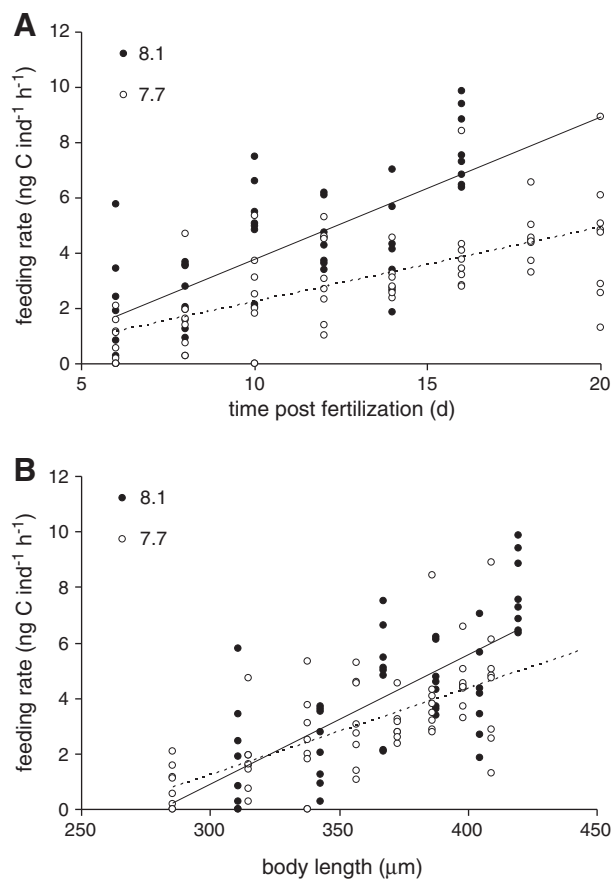

Fig. 6. Feeding rate (FR, ng C ind^{-1} h^{-1}) of larvae raised under control (black symbols, solid regression) and elevated pCO_2 (open symbols, dashed regression) plotted against time post-fertilization (A) and body length (B). Significant differences were observed between treatments when plotted against time post-fertilization (Table 3) but not when plotted against body length (Table 3). Regression equations and coefficients are listed in Table 2.
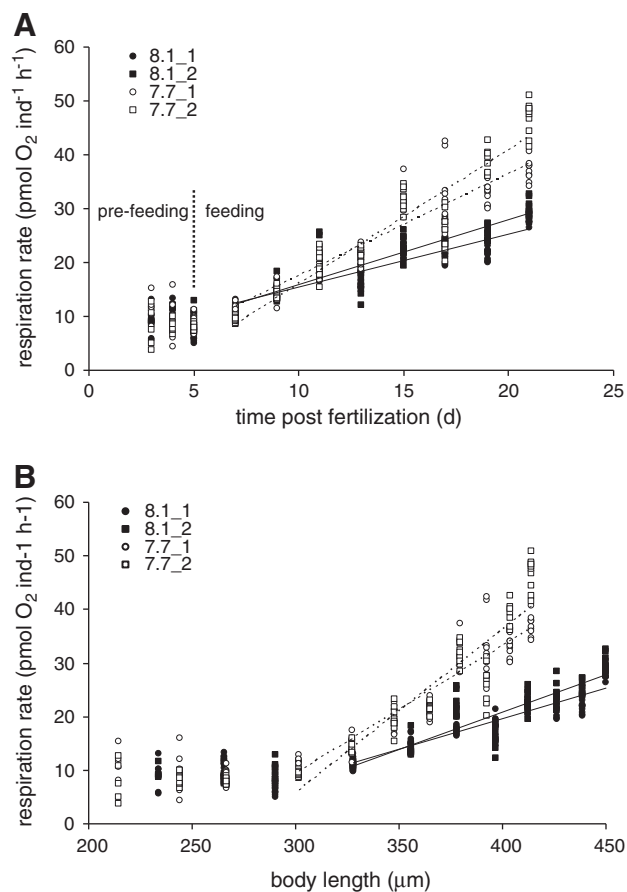

Fig. 7. Routine metabolic rates in dublicate cultures (RMR, pmol O$_2$ ind^{-1} h^{-1}) of larvae raised under control (black symbols, solid regression) and low pH conditions (open symbols, dashed regression) plotted against time post-fertilization (A) and body length (B). Vertical line indicates start of feeding. Significant difference between treatments was observed after feeding commences when plotting RMR against time post-fertilization (Table 3) as well as body length (Table 3). Regression equations and coefficients are listed in Table 2.

4. Discussion

This study revealed significant impacts of elevated seawater pCO_2 on the dynamic of survival, development, feeding and metabolism of *Strongylocentrotus purpuratus* larvae. Most recent studies examining sea urchin early development have focused only on development/ growth and gene expression patterns in unfed larvae (Kurihara and Shirayama, 2004; Kurihara, 2008; Clark et al., 2009; Todgham and Hofmann, 2009; Brennand et al., 2010; O'Donnell et al., 2010). Here and in our companion study (Stumpp et al., 2011) we show that the impact of simulated ocean acidification on sea urchin larvae is more pronounced in feeding vs. in pre-feeding or unfed stages, resulting in a developmental delay, elevated metabolic rates and changes in gene expression patterns. Feeding rate remain constant when normalized to body size (body length) as a reference scale rather than time post-fertilization. This enables differentiation between direct effects of climate change on larval morphology and physiology and indirect effects due to delayed development. Developmental delays appear to be primarily a consequence of altered energy budgets under altered abiotic stress regimes.

4.1. Impact of pCO_2 on survival

Survival seemed to be positively impacted by low pH when time post-fertilization was used as a reference point. When correcting to body length, survival rate was not impacted as strongly, but was
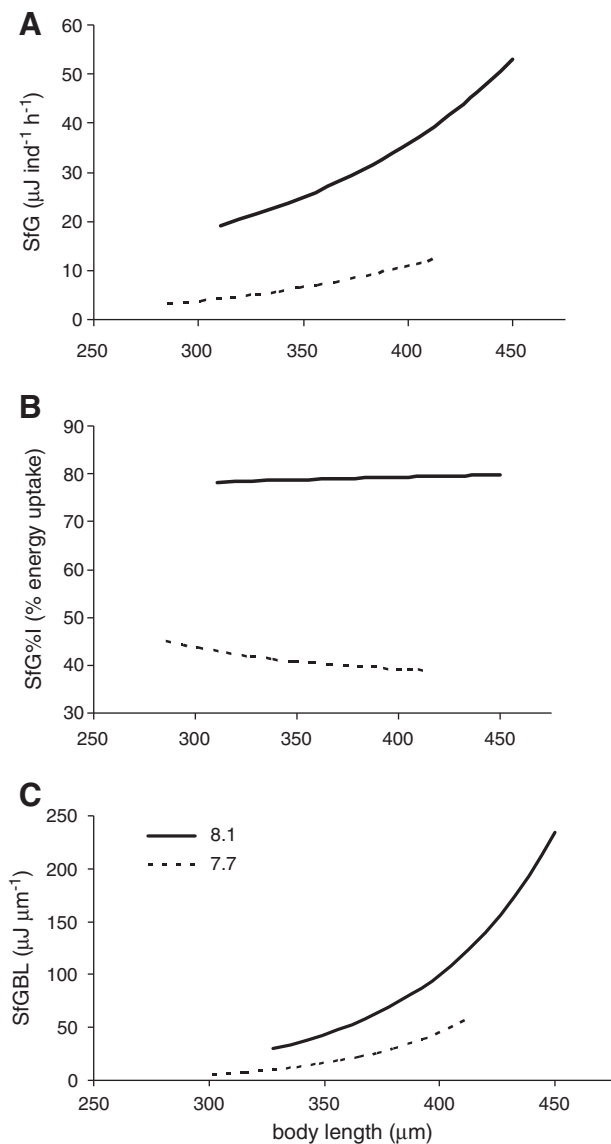
Fig. 8. Scope for growth (SfG) for larvae raised under control (solid line) and elevated pCO_2 (dashed line) conditions. SfG was calculated from metabolic and feeding rates and was normalized onto larval size assuming a reduced size of 8% under elevated pCO_2 conditions in comparison to control. A SfG (μJ ind^{-1} h^{-1}). B SfG$_{\%I}$ (% energy income). C SfG$_{BL}$ (μJ ind^{-1} μm^{-1}).

significantly higher than survival rate in control condition (by 11%). This is in contrast to larvae of the ophiuroid *Ophiotrix fragilis* which was characterized by 100% mortality at a seawater pCO_2 expected for the next 100–300 years (Dupont et al., 2008), but is in accordance with previous studies in a range of echinoids (*Tripneustes gratilla*, *Pseudechinus huttoni*, *Evechinus chloroticus*, *Sterechinus neumayeri*, *Echinus mathaei*, *Hemicentrotus erythrogramma*, *Hemicentrotus pulcherrimus*) where moderately elevated seawater pCO_2 (ca. 100–150 Pa) did not significantly alter mortality (Kurihara and Shirayama, 2004; Kurihara, 2008; Clark et al., 2009).

4.2. Impact of pCO_2 on growth, morphometrics and morphology

At a given time (TPF), we observed that rod and body lengths were smaller when larvae were raised under elevated pCO_2, compared to the control. This is in accordance with previous publications showing that an elevated pCO_2 resulted in smaller larvae at the same time post-fertilization (Kurihara and Shirayama, 2004; Kurihara, 2008; Clark et al., 2009; O'Donnell et al., 2010). When normalizing the different rod lengths to body length in order to correct for a potential growth delay, it became apparent that larvae raised under lower pH were not just smaller, but resemble the proportions encountered in earlier larval stages. This was confirmed by allometric comparisons. Antibody labeling of msp 130 and serotonin in 4 arm pluteus stage larvae revealed no impact of decreased seawater pH on differentiation of PMC cells or the nervous system. Development of skeletogenic cells (PMCs) and the nervous system appeared to be normal according to the 4 arm pluteus stage (Bisgrove and Burke, 1986; Yajima and Kiyomoto, 2006).

These decreased growth rates at elevated pCO_2 treatment in *S. purpuratus* and several other sea urchin species (*T. gratilla, P. huttoni, E. chloroticus, S. neumayeri, E. mathaei, H. erythrogramma, H. pulcherrimus*: Kurihara and Shirayama, 2004; Kurihara, 2008; Clark et al., 2009; Brennand et al., 2010; O'Donnell et al., 2010) are very likely potentiating the susceptibility of larval stages due to the high predation pressure in the pelagic environment (Hare and Cowen, 1997; Allen, 2008; Dupont et al., 2010a) and/or have negative effect on phenology, e.g. by delaying the opportunity to settle in a favorable habitat with high quality conditions (for example seasonal feeding conditions) (Miner, 2005; Elkin and Marshall, 2007). This may influence adult recruitment and community structure of populations in the future.

4.3. Impact of pCO_2 on feeding

In sea urchin larvae, the ciliary bands running along the larval arms are the feeding structures and feeding efficiency is then directly linked to arm length. Sea urchin larvae are extremely plastic and even before the gut is fully developed and ready to digest food, larval arms grow in length depending on the environmental food conditions (Strathmann, 1971; Miner, 2005).

In our experiment, food conditions were kept constant in the two pCO_2 treatment levels and could not alter growth of feeding structures between pH treatments. Feeding experiments revealed that when the developmental delay is ignored; feeding is apparently reduced in the high pCO_2 treatment. When considering the developmental delay, larvae from the two pCO_2 treatments of similar size are characterized by comparable feeding efficiency. As a consequence, the larvae are supplied with the same amount of energy for growth and maintenance under both pCO_2 levels. A correlation between larval morphology and physiological processes in response to hypercapnia was also found in *Paracentrotus lividus*: reduced calcification rate in response to elevated pCO_2 could be related to reduced growth rates. Skeletogenesis appeared to be normal when considering the developmental delay (Martin et al., 2011).

4.4. Impact of pCO_2 on aerobic metabolic rate and scope for growth

Routine metabolic rates increased after larvae began feeding which is in accordance with the literature for *S. purpuratus* and *Sterechinus neumayeri* (Marsh et al., 1999; Meyer et al., 2007). Our control respiration rates were in the range of published values for *S. purpuratus* (Meyer et al., 2007). Under elevated pCO_2 larval metabolic rates increased significantly when compared to those under control conditions (by 100%), an effect that increased in magnitude when correcting for the developmental delay. Previous studies have described a down regulation of metabolic genes in embryonic and unfed early 4-arm pluteus stages of *S. purpuratus* and *Lytechinus pictus* (Todgham and Hofmann, 2009; O'Donnell et al., 2010). In older, feeding *S. purpuratus* larvae, we found an up regulation of several metabolic genes, which is consistent with the increased metabolic rates observed in the current study (Stumpp et al., 2011).

Other studies on a range of marine invertebrates found metabolic depression under relatively high seawater pCO_2 values and suggested that uncompensated extracellular pH might be the trigger for these reductions (Langenbuch and Pörtner, 2002; Pörtner et al., 2004;

Michaelidis et al., 2005). However, using moderate levels of acidification, metabolic rates remained unchanged or increased under CO_2 induced acidification stress in a range of species, even when extracellular pH was decreased (Gutowska et al., 2008; Wood et al., 2008; Comeau et al., 2010; Thomsen et al., 2010; Thomsen and Melzner, 2010). An increase of metabolic rates under elevated seawater pCO_2 while growth and calcification rates were negatively impacted (Comeau et al., 2010; Thomsen and Melzner, 2010) points towards higher costs for the maintenance of cellular homeostasis and calcification processes.

Deigweiher et al. (2010) investigated CO_2 induced changes in gill energy budgets in Antarctic the notothenioid fish *Gobionotothen gibberifrons* and *Notothenia coriiceps* and found that energetic demands of processes such as protein synthesis and Na^+/K^+ ATPase activity were increasing while overall metabolic rates of gill tissues remained relatively constant under hypercapnia. The Na^+/K^+-ATPase, the main motor of cellular and extrallelular acid–base balance and thus an important ion regulatory player (Melzner et al., 2009) can account for 77% of total metabolic rate in *S. purpuratus* pluteus larvae and forty percent of respiratory energy alone is needed to maintain ion balance Leong and Manahan (1997). As it was found that Na^+/K^+-ATPase gene expression is upregulated under hypercapnic stress in purple sea urchin larvae (Stumpp et al., 2011) it is quite likely that Na^+/K^+-ATPase activity is increased with increasing environmental acid–base stress through CO_2 induced acidification. This could then increase routine metabolic rates under elevated pCO_2 conditions.

The increase in metabolic rate under elevated pCO_2 influences the energy balance calculated as scope for growth (SfG) in sea urchin larvae and can be correlated to the observed growth. SfG integrates physiological, cellular and biochemical changes to one response variable at the whole organism level and provides a robust tool for measuring whole animal performance under stress (Navarro et al., 2006). SfG has been shown to decrease due to a variety of stressors including temperature, salinity or pollution in a range of marine and freshwater invertebrates (Shirley and Stickle, 1982; Widdows and Johnson, 1988; Maltby et al., 1990; Gonzáles et al., 2002; Verslycke et al., 2004; Mubiana and Blust, 2007) either via decreased energy input (e.g. food intake), by increased energy loss (e.g. respiratory or excretory energy loss) or due to a combination of both. During sea urchin larval development, SfG increases exponentially with body length and in relation to the energy input SfG follows a saturation curve indicating that up to 61% of energy input can be allocated to growth/development after larvae start to feed.

Under elevated pCO_2, SfG is decreased by up to 50% depending on larval size. SfG follows an exponential decrease, which explains the reduced rates of development recorded. Further, the decrease in SfG during development indicates that maintenance seems to become increasingly energy consuming under hypercapnia. The energy that is supplied to grow a certain length increment increases exponentially under both conditions, which is related to rapid growth in volume. However, the energy supply to grow a defined size increment differs between treatments and highlights again, that larvae exposed to hypercapnic conditions face higher energetic demands to supply processes that are more vital on an acute basis: e.g. maintenance of cellular and extracellular homeostasis and/or maintenance of skeletal integrity. However, although gene transcription data points toward a higher need of ion regulatory activity (upregulation of Na^+/K^+-ATPase transcripts, Martin et al., 2011; Stumpp et al., 2011) and possibly skeletogenesis (upregulation of calcification gene transcripts in *P. lividus*, Martin et al., 2011), mechanistic data on processes that have to be fueled with additional energy is still lacking.

5. Conclusions

This study combined measurements of growth and developmental plasticity with routine metabolic and feeding rates to investigate the effects of simulated ocean acidification on *S. purpuratus* larval energy budgets. We suggest that body length is a useful scale of reference for studies in sea urchin larvae where a morphological delay in development occurs. Using time post-fertilization (TPF) as a reference may lead to misinterpretation of data. Utilizing routine metabolic and feeding rates we developed a scope for growth model (SfG) for sea urchin larvae. This is the first study that uses SfG to investigate the impact of elevated pCO_2 on larval energy budgets. We showed that for a given larval morphology, hypercapnia increases costs of maintenance and thus decreases SfG. However, to understand hypercapnia induced shifts in energy budgets and to pinpoint the processes that require more energy, studies focusing on ion regulatory capacity and acid–base homeostasis are needed.

Supplementary materials related to this article can be found online at doi:10.1016/j.cbpa.2011.06.022.

References

Allen, J.D., 2008. Size-specific predation on marine invertebrate larvae. Biol. Bull. 214, 42–49.

Anstrom, J.A., Chin, J.E., Leaf, D.S., Parks, A.L., Raff, R.A., 1987. Localization and expression of msp130, a primary mesenchyme lineage-specific cell surface protein in the sea urchin embryo. Development 101, 255–265.

Ben-Tabou de-Leon, S., Davidson, E.H., 2007. Gene regulation: gene control network in development. Annu. Rev. Biophys. Biomol. Struct. 36, 191–212.

Biermann, C.H., Kessing, B.D., Palumbi, S.R., 2003. Phylogeny and development of marine model species: strongylocetrotid sea urchins. Evol. Dev. 5, 360–371.

Bisgrove, B.W., Burke, R.D., 1986. Development of serotonergic neurons in embryos of the sea urchin *Strongylocentrotus purpuratus*. Dev. Growth Differ. 28, 569–574.

Brennand, H.S., Soars, N., Dworjanyn, S.A., Davis, A.R., Byrne, M., 2010. Impact of ocean warming and ocean acidification on larval development and calcification in the sea urchin *Tripneustes gratilla*. Plos One 5, e11372.

Clark, D., Lamare, M., Barker, M., 2009. Response of sea urchin pluteus larvae (Echinodermata: Echinoidea) to reduced seawater pH: a comparison among tropical, temperate, and a polar species. Mar. Biol. 156, 1125–1137.

Comeau, S., Jeffree, R., Teyssie, J.L., Gattuso, J.P., 2010. Response of the Arctic Pteropod *Limacina helicina* to projected future environmental conditions. Plos One 5, e11362.

Deigweiher, K., Hirse, T., Bock, C., Lucassen, M., Pörtner, H.-O., 2010. Hypercapnia induced shifts in gill energy budgets of Antarctic notothenioids. J. Comp. Physiol. B 180, 347–359.

Dickson, A.G., Millero, F.J., 1987. A comparison of the equilibrium constants for the dissociation of carbonic acid in seawater media. Deep-Sea Res. 34, 1733–1743 (Corrigenda. Deep-Sea Res. 1736, 1983).

Doney, S.C., Fabry, V.J., Feely, R.A., Kleypas, J.A., 2009. Ocean acidification: the other CO_2 problem. Annu. Rev. Mar. Sci. 1, 169–192.

Dupont, S., Dorey, N., Thorndyke, M., 2010a. What meta-analysis can tell us about vulnerability of marine biodiversity to ocean acidification? Estuarine Coastal Shelf Sci. doi:10.1016/j.ecss.2010.06.013.

Dupont, S., Havenhand, J., Thorndyke, W., Peck, L., Thorndyke, M.C., 2008. CO_2-driven ocean acidification radically affect larval survival and development in the brittlestar *Ophiotrix fragilis*. Mar. Ecol. Prog. Ser. 373, 285–294.

Dupont, S., Lundve, B., Thorndyke, M., 2010b. Near future ocean acidification increases growth rate of the lecithotrophic larvae and juveniles of the sea star *Crossaster papposus*. J. Exp. Zool. B 314B, 382–389.

Dupont, S., Ortega-Martínez, O., Thorndyke, M.C., 2010c. Impact of near-future ocean acidification on echinoderms. Ecotoxicology 19, 449–462.

Ebert, T.A., 1967. Negative growth and longevity in the purple sea urchin *Strongylocentrotus purpuratus* (Stimpson). Science 157, 557–558.

Elkin, C., Marshall, D.J., 2007. Desperate larvae: influence of deferred costs and habitat requirements on habitat selection. Mar. Ecol. Prog. Ser. 335, 143–153.

Frost, B.W., 1972. Effects of size and concentration of food particles on the feeding behaviour of the marine planktonic copepod *Calanus pacificus*. Limnol. Oceanogr. 17, 805–815.

Gnaiger, E., 1983. Calculation of Energetic and Biochemical Equivalents of Respiratory Oxygen Consumption. In: Gnaiger, E., Forstner, H. (Eds.), Polarographic Oxygen Sensors: Aquatic and Physiological Applications. Springer-Verlag, New York.

Gonzáles, M.L., López, D.A., Pérez, M.C., Castro, J.M., 2002. Effect of temperature on the scope for growth in juvenile scallops *Artopecten purpuratus* (Lamark, 1819). Aquacult. Int. 10, 339–349.

Guillard, R.R.L., Ryther, J.H., 1962. Studies of marine planktonic diatoms. I. *Cyclotella nana* Husted, and *Detonula confervacea* (Cleve). Can. J. Microbiol. 8, 229–239.

Gutowska, M.A., Pörtner, H.-O., Melzner, F., 2008. Growth and calcification in the cephalopod *Sepia officinalis* under elevated seawater pCO_2. Mar. Ecol. Prog. Ser. 373, 303–309.

Hare, J.A., Cowen, R.K., 1997. Size, growth, development, and survival of the planktonic larvae of *Pomatomus saltatrix* (Pisces: Pomatomidae). Ecology 78, 2415–2431.

Kroeker, K.J., Kordas, R.L., Crim, R.N., Singh, G.G., 2010. Meta-analysis reveals negative yet variable effects of ocean acidification on marine organisms. Ecol. Lett. 13, 1419–1434.

Kurihara, H., 2008. Effects of CO_2-driven ocean acidification on the early developmental stages of invertebrates. Mar. Ecol. Prog. Ser. 373, 275–284.

Kurihara, H., Shirayama, Y., 2004. Effects of increased atmospheric CO_2 on sea urchin early development. Mar. Ecol. Prog. Ser. 274, 161–169.

Langenbuch, M., Pörtner, H.O., 2002. Changes in metabolic rate and N excretion in the marine invertebrate *Sipunculus nudus* under conditions of environmental hypercapnia: identifying effective acid–base variables. J. Exp. Biol. 205, 1153–1160.

Leong, P.K.K., Manahan, D.T., 1997. Metabolic importance of Na^+/K^+-ATPase activity during sea urchin development. J. Exp. Biol. 200, 2881–2892.

Lewis, E., Wallace, D.W.R., 1998. CO2SYS—Program Developed for the CO_2 System Calculations. Carbon Dioxide Inf Anal Center Report ORNL/CDIAC-105.

Maltby, L., Naylor, C., Calow, P., 1990. Effect of stress on a freshwater benthic detritivore: scope for growth in *Gammarus pulex*. Ecotoxicol. Environ. Saf. 19, 285–291.

Marsh, A.G., Leong, P.K.K., Manahan, D.T., 1999. Energy metabolism during embryonic development and larval growth of an antarctic sea urchin. J. Exp. Biol. 202, 2041–2050.

Marsh, A.G., Manahan, D.T., 1999. A method for accurate measurements of the respiration rates of marine invertebrate embryos and larvae. Mar. Ecol. Prog. Ser. 184, 1–10.

Martin, S., Richier, S., Pedrotti, M.-L., Dupont, S., Castejon, C., Gerakis, Y., Kerros, M.-E., Oberhänsli, F., Teyssié, J.-L., Gattuso, J.P., 2011. Early development and molecular plasticity in the Mediterranean sea urchin *Paracentrotus lividus* exposed to CO_2 driven ocean acidification. J. Exp. Biol. 214, 1357–1368.

Mehrbach, C., Culberson, C.H., Hawley, J.E., Pytkowicz, R.M., 1973. Measurement of the apparent dissociation constants of carbonic acid in seawater at atmospheric pressure. Limnol. Oceanogr. 18, 897–907.

Melzner, F., Gutowska, M.A., Langenbuch, M., Dupont, S., Lucassen, M., Thorndyke, M.C., Bleich, M., Pörtner, H.-O., 2009. Physiological basis for high CO_2 tolerance in marine ectothermic animals: pre-adaptation through lifestyle and otogeny? Biogeosciences 6, 2313–2331.

Meyer, E., Green, A.J., Moore, M., Manahan, D.T., 2007. Food availability and physiological state of sea urchin larvae (*Strongylocentrotus purpuratus*). Mar. Biol. 152, 179–191.

Michaelidis, B., Ouzounis, C., Paleras, A., Pörtner, H.-O., 2005. Effects of long-term moderate hypercapnia on acid–base balance and growth rate in marine mussels *Mytilus galloprovincialis*. Mar. Ecol. Prog. Ser. 293, 109–118.

Miner, B.G., 2005. Evolution of feeding structure plasticity in marine invertebrate larvae: a possible trade-off between arm length and stomach size. J. Exp. Mar. Biol. Ecol. 315, 117–125.

Mubiana, V.K., Blust, R., 2007. Effects of temperature on scope for growth and accumulation of Cd, Co, Cu and Pb by the marine bivalve *Mytilus edulis*. Mar. Environ. Res. 63, 219–235.

Mullin, M.M., Sloan, P.R., Eppley, R.W., 1966. Relationship between carbon content, cell volume, and area in phytoplankton. Limnol. Oceanogr. 11, 307–311.

Navarro, J.M., Urrutia, G.X., Carrasco, C., 2006. Scope for growth versus actual growth in the juvenile predatory gastropod *Chorus giganteus*. J. Mar. Biol. Assoc. U. K. 86, 1423–1428.

O'Donnell, M.J., Todgham, A.E., Sewell, M.A., Hammond, L.M., Ruggiero, K., Fangue, N.A., Zippay, M.L., Hofmann, G.E., 2010. Ocean acidification alters skeletogenesis and gene expression in larval sea urchins. Mar. Ecol. Prog. Ser. 398, 157–171.

Okazaki, K., Inoué, S., 1976. Crystal property of the larval sea urchin spicule. Dev. Growth Differ. 18, 413–434.

Orr, J.C., Fabry, V.J., Aumont, O., Bopp, L., Doney, S.C., Feely, R.A., Gnanadesikan, A., Gruber, N., Ishida, A., Joos, F., Key, R.M., Lindsay, K., Maier-Reimer, E., Matear, R., Mofray, P., Mouchet, A., Najjar, R.G., Plattner, G.-K., Rodgers, K.B., Sabine, C.L., Sarmiento, J.L., Schlitzer, R., Slater, R.D., Totterdell, I.J., Weirig, M.-F., Yamanaka, Y., Yool, A., 2006. Anthropogenic ocean acidification over the twenty-first century and its impact on calcifying organisms. Nature 437, 681–686.

Pearse, J.S., 2006. Ecological role of purple sea urchins. Science 314, 940–941.

Pörtner, H.-O., Dupont, S., Melzner, F., Storch, D., Thorndyke, M., 2010. Studies of Metabolic Rate and Other Characters Across Life Stages. In: Riebesell, U., Fabry, V.J., Hansson, L., Gattuso, J.-P. (Eds.), Guide to Best Practices for Ocean Acidification Research and Data Reporting. Publications Office of the European Union, Luxembourg, pp. 167–180.

Pörtner, H.O., Langenbuch, M., Reipschläger, A., 2004. Biological impact of elevated ocean CO_2 concentrations: lessons from animal physiology and earth history. J. Oceanogr. 60, 705–718.

Renaud, S.M., Thinh, L.V., Lambrinidis, G., Parry, D.L., 2002. Effect of temperature on growth, chemical composition and fatty acid composition of tropical Australian microalgae grown in batch cultures. Aquaculture 211, 195–214.

Sarazin, G., Michard, G., Prevot, F., 1999. A rapid and accurate spectroscopic method for alkalinity measurements in seawater samples. Water Res 33, 290–294.

S.A.S. Institute, 1990. SAS/STAT User's guide. SAS Institute. Vol.

Sea Urchin Genome Sequencing Consortium, 2006. The genome of the sea urchin *Strongylocentrotus purpuratus*. Science 314, 941–952.

Shapiro, S.S., Wilk, M.B., 1965. An analysis of variance test for normality. Biometrika 52, 591–599.

Shilling, F.M., Manahan, D.T., 1994. Energy metabolism and amino acid transport during early development of antarctic and temperate echinoderms. Biol. Bull. 187, 398–407.

Shirley, T.C., Stickle, W.B., 1982. Responses of *Leptasterias hexactis* (Echinodermata: Asteroidea) to low salinity II. Nitrogen metabolism, respiration and energy budget. Mar. Biol. 69, 155–163.

Smith, M.M., Smith, L.C., Cameron, A., Urry, L.A., 2008. The larval stages of the sea urchin, *Strongylocentrotus purpuratus*. J. Morphol. 269, 713–733.

Steneck, R.S., Graham, M.H., Bourque, B.J., Corbett, D., Erlandson, J.M., Estes, J.A., Tegner, M.J., 2002. Kelp forest ecosystems: biodiversity, stability, resilience and future. Environ. Conserv. 29, 436–459.

Strathmann, R.R., 1971. The feeding behavior of planktotrophic echinoderm larvae: mechanisms, regulation, and rates of suspension feeding. J. Exp. Mar. Biol. Ecol. 6, 109–160.

Stumpp, M., Dupont, S., Thorndyke, M.C., Melzner, F., 2011. CO_2-induced seawater acidification impacts sea urchin larval development II: gene expression patterns in pluteus larvae. Comp. Biochem. Physiol. A. 160, 320–330.

Thomsen, J., Gutowska, M.A., Saphörster, J., Heinemann, A., Fietzke, J., Hiebenthal, C., Eisenhauer, A., Körtzinger, A., Wahl, M., Melzner, F., 2010. Calcifying invertebrates succeed in a naturally CO_2 enriched coastal habitat but are threatened by high levels of future acidification. Biogeosciences 7, 3879–3891.

Thomsen, J., Melzner, F., 2010. Seawater acidification does not elicit metabolic depression in the blue mussel *Mytilus edulis*. Mar. Biol. 157, 2667–2676.

Todgham, A.E., Hofmann, G.E., 2009. Transcriptomic response of sea urchin larvae *Strongylocentrotus purpuratus* to CO_2-driven seawater acidification. J. Exp. Biol. 212, 2579–2594.

Verslycke, T., Roast, S.D., Widdows, J., Jones, M.B., Janssen, C.R., 2004. Cellular energy allocation and scope for growth in the estuarine mysid *Neomysis integer* (Crustacea : Mysidacea) following chlorpyrifos exposure: a method comparison. J. Exp. Mar. Biol. Ecol. 306, 1–16.

Widdows, J., Johnson, D., 1988. Physiological energetics of *Mytilus edulis*: scope for growth. Mar. Ecol. Prog. Ser. 46, 113–121.

Wood, H.L., Spicer, J.I., Widdicombe, S., 2008. Ocean acidification may increase calcification rates, but at a cost. Proc. R. Soc. B Biol. 275, 1767–1773.

Yajima, M., Kiyomoto, M., 2006. Study of larval and adult skeletogenic cells in developing sea urchin larvae. Biol. Bull. 211, 183–192.